



## GAS Filter Tuning in AEI 10m Prototype

Kevin Aris\*

*Max Planck Institute for Gravitational Physics,*

*Leibniz University, Hannover, Germany and*

*Department of Physics, University of Florida, Gainesville, FL, USA*

(Dated: August 10, 2015)

### Abstract

At the Albert Einstein Institute (AEI) in Hannover, Germany, an interferometer with an arm length of approximately 10 meters is being set up for the testing and development of noise attenuation systems for future gravitational wave detectors. Additionally, the prototype will be used for testing high precision measurements such as the SQL (Standard Quantum Limit). The interferometer is housed in a large vacuum system and all of the optics in vacuum are mounted on one of three seismically isolated optical tables. The seismic isolation of these tables is achieved by 3 inverted pendulums and 3 geometric anti-spring (GAS) filters. These inverted pendulum legs and GAS filters are mechanical low-frequency oscillators that work passively to reduce seismic noise. The IP flexures achieve isolation in the horizontal direction and the GAS filters isolate in the vertical direction. Additionally, a system of sensors and actuators is present in the tables to provide active attenuation. The focus of my research while at the AEI was tuning the GAS filters to their lowest possible resonance frequency (Approximately 0.2 - 0.3 Hz).

## I. INTRODUCTION: GRAVITATIONAL WAVES

Gravitational waves were predicted in Einstein's Theory of General Relativity in 1916. By thinking of spacetime as a fabric on which masses sit, gravitational waves can be thought of as oscillatory perturbations in that fabric that manifest as fluctuating tidal forces on masses. These perturbations can be caused by the movement of asymmetrical masses in space or by the orbit of masses around one another. Gravitational waves are caused by oscillating multipole moments within these systems. They are transverse and they move at the speed of light. The gravitational waves cannot be monopole or dipole in character due to conservation of mass and conservation of angular momentum, respectively. Therefore, the leading term must be quadrupole [2]. The fact that gravitational waves are quadrupole waves means that the disturbances they cause in spacetime occur orthogonal to their direction of propagation. This disturbance manifests itself as a contraction along one orthogonal axis and an expansion along the other orthogonal axis. In other words, if you imagine a gravitational wave is propagating along the z-axis, it causes oscillating expansions and contractions along the x-axis and y-axis (See Figure 1).

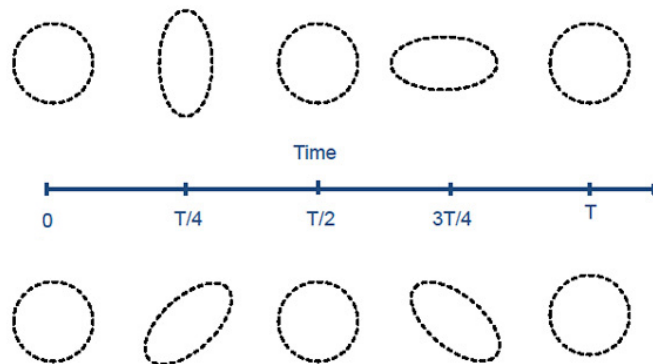


FIG. 1: Here is an image of the process described above as gravitational waves propagate into or out of the page. The bottom row is simply the first row with the x-axis and y-axis rotated 45 degrees and it represents the second of the two polarizations.

This interaction with the surrounding matter is very weak and therefore very difficult to detect. The strength of the fabric of spacetime makes it difficult for even the most massive of stellar objects to cause a discernible disturbance.

The detection of gravitational waves is important because they will provide another form of information we can get from cosmic activities. Additionally, it would prove that Einstein's theory of General Relativity was correct. Currently, we can only observe stellar events and

objects using electromagnetic radiation. This can give us information on most phenomena but gravitational waves will provide more insight into the behavior of massive systems such as black holes, white dwarfs and neutron stars. These can be observed because they are the only systems that produce gravitational waves with large enough amplitudes to be detected. No gravitational waves have been observed yet but indirect evidence of their existence has been gathered. In an experiment done by Hulse and Taylor, evidence of the existence of gravitational waves was observed through a system of two neutron stars orbiting one another. One of these neutron stars was a pulsar. Using the radio wave pulses as a tool, Hulse and Taylor tracked the orbital decay of the binary system. They found that the rate of orbital decay was accurately depicted by the emission of gravitational waves [4].

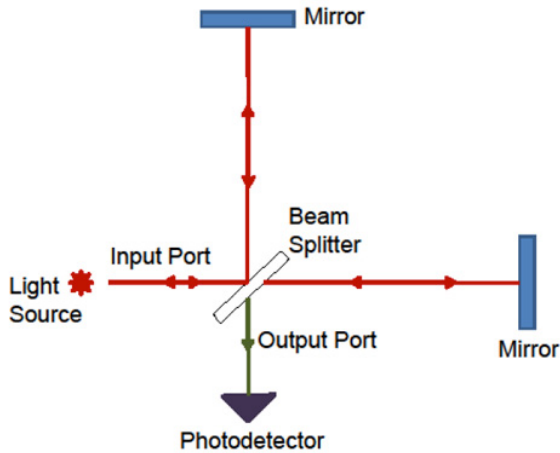
## II. INTERFEROMETRY

Numerous methods for the detection of gravitational wave detection have been proposed by the most promising of these methods is interferometry. A Michelson interferometer (See Figure 2) consists of a laser beam being split into two orthogonal arms. At the ends of these arms are mirrors. After the two orthogonal beams are reflected off of these mirrors, they recombine at the beam splitter. The recombined light then travels to the photodiode and an interference pattern is observed. The differential movement of the arms due to gravitational waves then causes changes in the interference pattern.

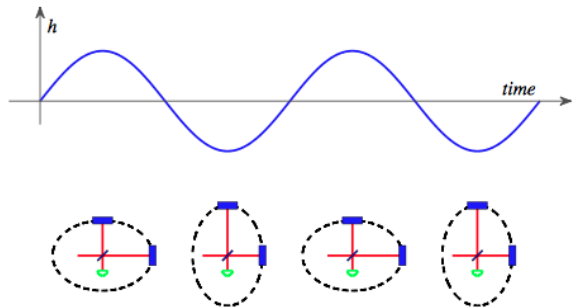
However, the magnitude of this differential movement of the interferometer arms due to gravitational waves is approximately  $10^{-18}$  meters. This means that all noise must be reduced to increase the signal to noise ratio. Current detectors include, but are not limited to, LIGO in the USA, VIRGO in Italy, and GEO600 in Germany. LIGO and VIRGO are currently in the process of being upgraded to advanced LIGO and advanced VIRGO. In addition to these two advanced detectors, KAGRA is being built in Japan[4].

## III. NOISE

Major noise sources for interferometers include seismic noise, quantum noise and thermal noise (See Figure 3). Temperature shifts can cause noise in many aspects of the interferometer system. Thermal fluctuations can cause unwanted imperfections in the mirror coatings



(a) This is a basic schematic of an interferometer. As a gravitational wave propagates through the arms, the differential movement causes phase modulations in the arms. This causes intensity modulations at the photodiode.



(b) The relation between the transverse gravitational wave and the interferometer arm modulation can be seen here. The amplitude  $h$  of the gravitational waves dictates the magnitude of the modulation.

FIG. 2

and the mirror substrates. Additionally, temperature fluctuations can cause unwanted vibrations in the wires that the mirrors are suspended from. Thermal noise is mainly seen in the frequency range from about 20Hz to 100Hz. Quantum noise has two major sources. One source is fluctuation in detected photons at the photodiode. Another source is vibrations of the mirror position caused by the impulse of the incident photons. This noise is mostly seen in higher frequencies. Seismic noise has a large number of sources. These include human activity, wind patterns, tide changes, small earthquakes, etc. Seismic waves dominate the noise at low frequency. These very low frequency oscillations are very hard to isolate and are the reason that the GAS filters and inverted pendulums must have very low resonance frequencies [4].

#### IV. AEI-SAS

At the AEI 10m Prototype, a seismic attenuation system (SAS) has been put in place to reduce the effect of seismic noise on measurements. The AEI-SAS consists of 3 inverted pendulum legs and 3 GAS filters for passive isolation. Passive isolation using harmonic isolators is achieved by making the resonance frequency of the oscillators as low as possible (Below 0.3Hz in this case). If an input signal of high frequency is incident on a harmonic

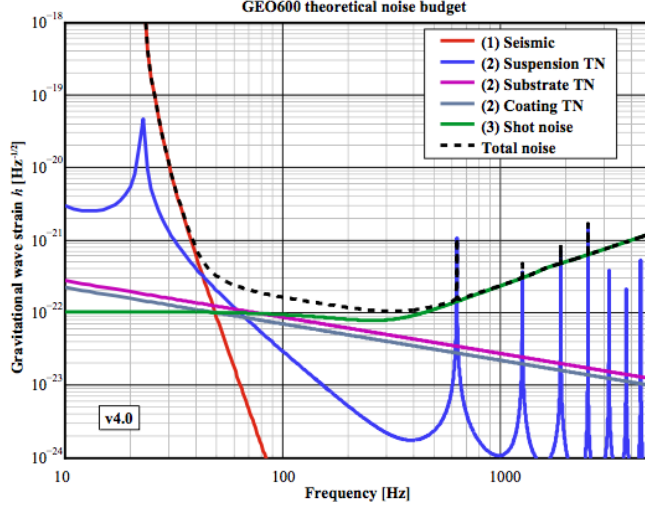


FIG. 3: This is a theoretical noise budget for the GEO600 detector in Germany. The domination of the noise at low frequencies of the seismic waves can be seen in the red line. The increasing quantum noise (shot noise) at high frequencies is indicated by the green line.

oscillator with a low resonance frequency, the harmonic oscillator will isolate its payload from the input signal. In addition, a system of sensors and actuators have been placed in the AEI-SAS tables for the purpose of monitoring the position of the tables and providing active attenuation. The inverted pendulums isolate in the horizontal direction. They are ideal for low frequency isolation because their resonance frequency can be driven much lower than a normal pendulum. In order to drive the resonance frequency of a traditional pendulum very low, the pendulum must be extremely long (using  $\omega = (g/l)^{1/2}$  where  $\omega$  is resonance frequency,  $g$  is acceleration due to gravity, and  $l$  is the pendulum length). For example, to achieve a resonance frequency of 0.2 Hz, a traditional pendulum would have to be approximately 50 meters in length. This is not feasible for laboratory experiments, especially in vacuum. Inverted pendulums can have very low resonance frequencies at laboratory feasible lengths. This is because when the inverted pendulum is displaced from equilibrium, gravity works to bring it further from equilibrium. This means that the force bringing the inverted pendulum back to equilibrium must overcome gravity (See Figure 4).

The GAS filters isolate in the vertical direction. They consist of 8 blade springs that are bent, then radially compressed. The Geometric Anti-Spring effect (See Figure 5) reduces the resonance frequency of the GAS filter by providing a force in the direction opposed to equilibrium. If a traditional spring were to have the low resonance frequency achieved by the GAS filters, it would have to have a very low spring constant (using  $\omega = (k/m)^{1/2}$  where  $\omega$

is resonance frequency,  $k$  is the spring constant, and  $m$  is the mass of the suspended object). However, with a very low spring constant, the spring would be extremely soft and small forces would cause a very large disturbance of the attached mass (Using  $F = -kx$  where  $F$  is the indecent force,  $k$  is the spring constant, and  $x$  is distance). The Inverted pendulums, GAS filters, sensors and actuators are all housed in large AEI-SAS tables (See Figure 6). In total, the entire system provides isolation in all 6 degrees of freedom ( $x$ ,  $y$ ,  $z$ , roll, pitch, and yaw) [6].

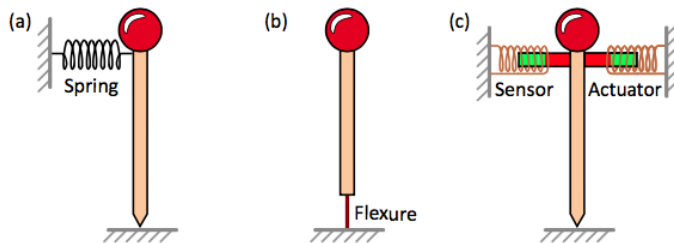


FIG. 4: Here are 3 different models for stabilizing inverted pendulums. Model (b) is the model used to design the inverted pendulums in the AEI-SAS. If no springs or flexures were involved the system would be inherently unstable. If no restoring force (springs and flexures) was present, the inverted pendulum would simply fall over if disturbed. Gravity would pull it to the ground is there was nothing to oppose it. The springs/flexures provide a for opposing gravity.

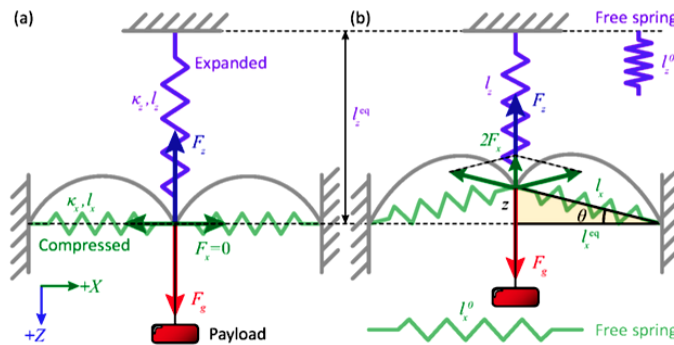
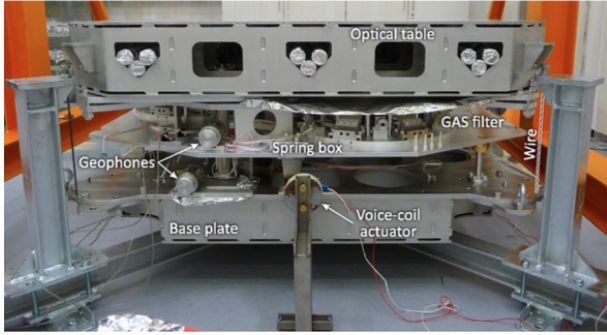
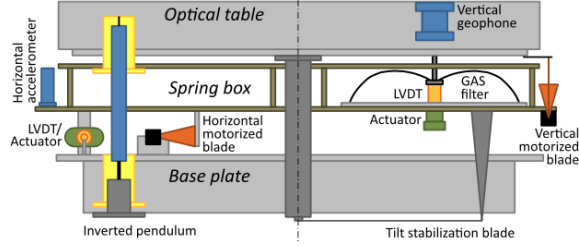


FIG. 5: The effective forces of the blade springs in the GAS filters (Grey) can be modeled by the 3 springs seen above (Green and Purple). As you can see in the second image, the horizontal springs in the model exert a force upward when the system is disturbed. This force makes opposes the downward force of the purple spring, which wants to being the system back to equilibrium. Thus, the system is slower to go back to equilibrium than if only the purple spring was present. This makes the resonance frequency of the blade spring system much lower than that of a traditional spring.

In addition to the active attenuation provided by the sensors and actuators, there is the suspension platform interferometer (SPI) on the center table (See Figure 7). The SPI consists of four interferometers and is used to attenuate the low frequency differential motion in the two major interferometer arms. The SPI components are mounted on a low thermal expansion Zerodur plate to reduce thermal noise.



(a) Each one of the 3 AEI-SAS tables consists of 3 GAS filters and 3 Inverted Pendulums with a variety of additional components. This is a side view of one of the tables. It is difficult to see some of the components of the table once it is full assembled so a schematic diagram is displayed to the right.



(b) The basic layout of the tables can be easily seen in this diagram. LVDT's (Linear Variable Differential Transformers) are sensors that measure differential motion between the ground and the table in a single dimension. The system of accelerometers, motorized blade springs, and LVDT's provide active attenuation through a feedback loop. The GAS filters are housed in the spring box that is supported by the 3 inverted pendulum legs. This image shows a third of the components of the table. All of these components exist 120 degrees from one another inside of the table.

FIG. 6

## V. GAS FILTER ASSEMBLY AND MATERIALS

The GAS filter blades are made of a special kind of steel called maraging steel. This is steel that has been artificially aged through a special kind of annealing process. This is done to the blades to reduce creep noise [6]. In its simplest terms, creep noise is caused by deformations in the crystal lattice of the steel due to prolonged stress. After the steel is aged, it is nickel plated to protect the blade from corrosion. An additional heating is done after the nickel plating in order to reduce the effect of hydrogen embrittlement (See Figure 8) on the steel. Hydrogen embrittlement is the weakening of steel at the points of highest stress due to Hydrogen atoms infiltrating the atomic structure of the metal [7]. The formation of metal hydrides at the points of highest stress in the steel causes micro fractures that can expand and lead to breaks over time. However, this process is not completely understood so it is difficult to completely remove the hydrogen from the blades. It is known that a relatively low baking temperature (approximately 200 degrees Celsius) reduces the effect by increasing the diffusion of hydrogen out of the steel, but this is only a temporary solution unless the blades are properly sealed in nickel.

Once the blades have been treated and annealed properly, they are assembled into the GAS filter configuration (See Figure 9) using a special tool. This tool makes sure that all

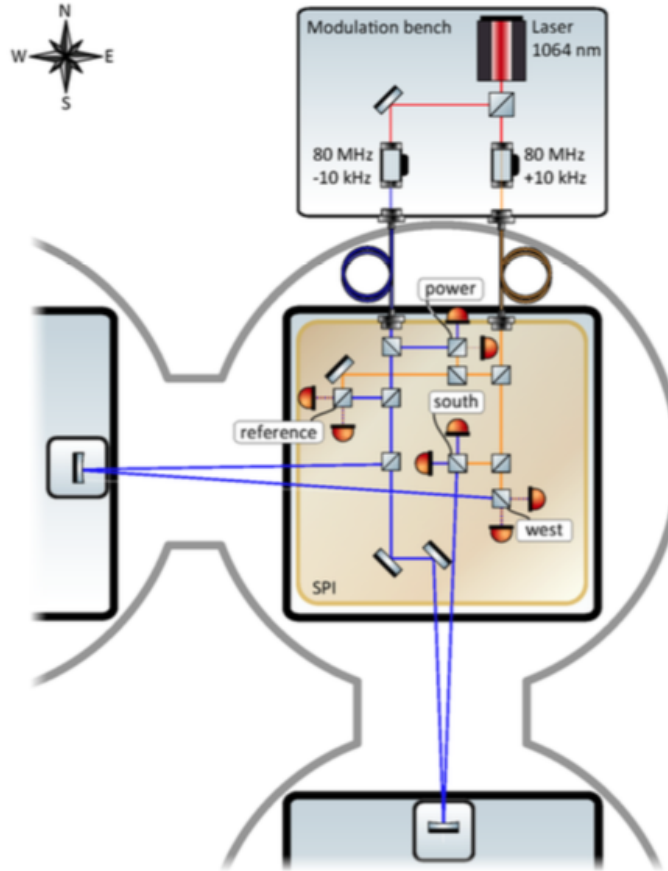
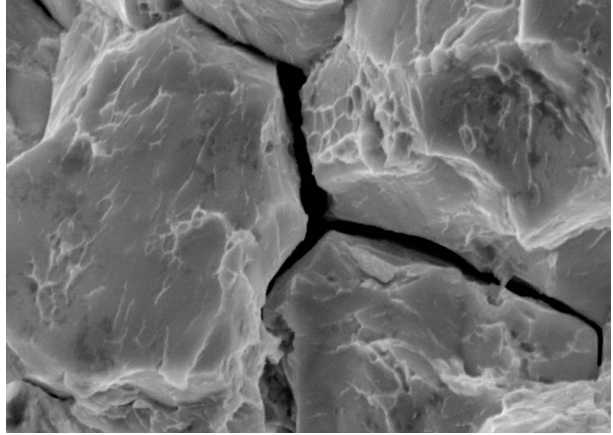
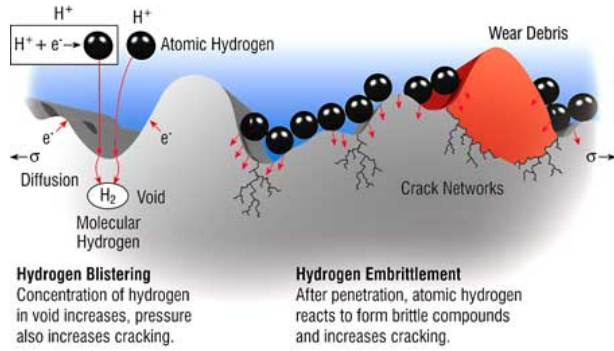


FIG. 7: This is a diagram of the SPI. In this diagram, the size of the setup is greatly exaggerated for visual purposes. The four interferometers involved are the power interferometer, the reference interferometer, and the two arm interferometers. The power interferometer is used for stabilization and diagnostics. The reference interferometer cancels common mode fluctuations. The other two interferometers measure the differential displacement of the south and west tables from the central table.

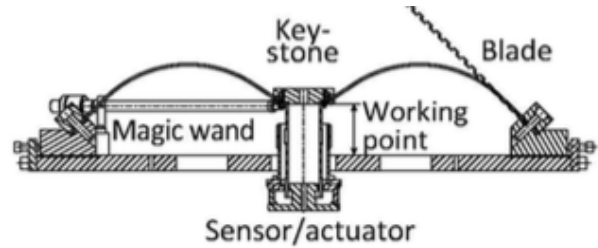
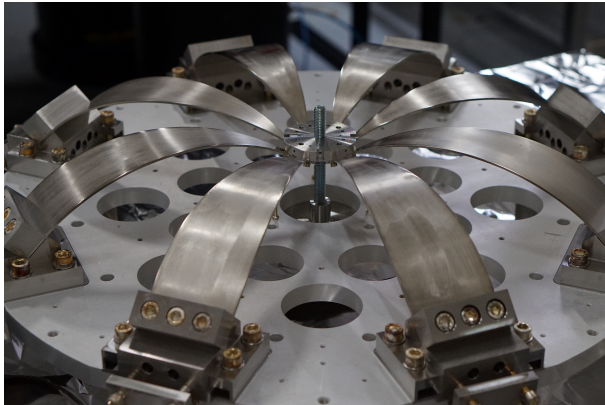
of the blades have the same radius of curvature. The blades are attached to the keystone in pairs to maintain balanced forces. Once all of the 8 blades have been attached to the keystone, the target length of the working point is approximately 85mm. This point is set as the zero point for the LVDT's that are attached to the GAS filter. The actuator that is attached to the GAS filter can then make small adjustments using a feedback loop that includes the LVDT. The base plate and the keystone of the GAS filters are cut from aluminum.



(a) This diagram of hydrogen embrittlement gives a brief explanation of how hydrogen weakens and penetrates the metal. Due to the fact that this process only requires metal to be in contact with hydrogen, it is very difficult to avoid unless the steel is always kept in vacuum or properly sealed with a nickel coating.

(b) This is a microscopic view of a metal surface affected by hydrogen embrittlement. The cracks cause by hydrogen embrittlement can be seen very well in this photo. The microscopic cracks can lead to macroscopic cracking and breaks in the metal.

FIG. 8



(a) The GAS filters are assembled in the configuration above. The blades are connected in pairs to the centerpiece (the keystone) to balance each other out.

(b) A schematic of the GAS filter to the left. The only difference is that the magic wands have not yet been added to the GAS filter on the left. The sensors and actuators on the bottom of the filter can be used to monitor and attenuate fluctuations in the working point. The wavy line shows the original position of the blade spring before it is bent.

FIG. 9

## VI. GAS FILTER SHAKER STAND TUNING

Once the GAS filter has been assembled as shown in Figure 9, it is ready for resonance tuning. To begin this process, the GAS filter has to be put into the GAS filter shaker test stand (See Figure 10). This stand is an aluminum cage from which the GAS filter can be hung by 4 commercial garage springs. These springs allow the GAS filter to freely oscillate. A payload that is comparable to a third of the weight of the optical table is then attached

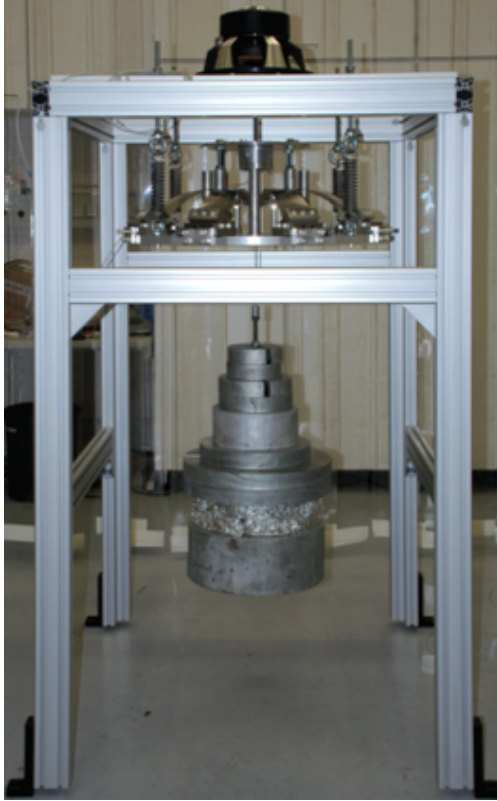


FIG. 10: All of the components of the shaker test stand are shown here. On top of the cage and connected to the filter is the subwoofer. The filter is connected to the stand using commercial grade garage springs. The amplifier drives the subwoofer on top with different frequencies and a transfer function is taken for the excitations provided by the subwoofer.

to the keystone. In order to drive the GAS filter at a range of frequencies (Approximately 0.1 - 100 Hz) a commercial subwoofer and amplifier are used. This subwoofer is bolted to the top of the shaker stand and the membrane is attached to the GAS filter. Two geophones are used to monitor the movement of the base plate and the payload mass. A geophone is a type of inertial sensor that can measure the oscillations of the object that it is attached to in a single dimension. In this case, one of the geophones is placed on the the base plate of the GAS filter and the other is placed on the bottom of the test mass. The ratio of the measurements of these two geophones represents the transfer function of the GAS filter. A transfer function is a relation between the input and the output of a system. It is defined as the Fourier transform of the output signal divided by the Fourier transfer of the input signal [4]. In order to test the function and location of the geophones, a real time measurement was taken from each one (See Figure 11). Furthermore, the real time measurement can be used to help confirm the resonance frequency given by a transfer function.

Once the shaker stand is completely set up and the geophone locations are known, the tuning process can begin. The amplifier that was used for the excitations did not function very well at low frequencies. It had a highpass filter at approximately 5 Hz. Below an input

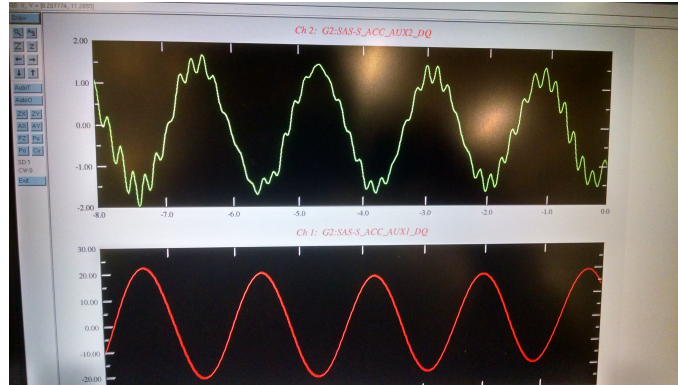


FIG. 11: This real time data gives us initial information about which geophone is on top and which is on bottom. As you can see from the two graphs, the green line represents the geophone on the GAS filter base plate and the red line represents the geophone on the bottom of the test mass. This is because the GAS filter is damping the high frequency noise that can be seen in the green line. This results in a much smoother, low frequency signal from the geophone on the bottom of the test mass. The transfer function that is measured is a way to measure the isolation seen here over a range of frequencies.

signal of 5 Hz, the amplifier output response lost the desired sinusoidal characteristics. Therefore, the ground motion caused by seismic activity was used as the excitation at low frequencies. This made it difficult to achieve a satisfactory level of coherence. Coherence describes the relationship between the phases of two signals. A high coherence between two signals means that their phase difference remains constant [8]. In order to counteract the low coherence, the real time data was monitored to make sure that the resonance frequency given by the transfer function matched the movement of the geophone attached to the test mass.

The GAS filters are tuned by tightening screws that face radially inward on the end of each blade (See Figure 12). With each turn, the blades get slightly more compressed. Additionally, the blades must be compressed in pairs so that the forces on the keystone remain balanced. As an additional precaution to keep the forces on the keystone balanced, the stress of each individual blade was measured before tuning. This was done by lightly striking each blade with an allen key and measuring the internal resonance frequency with a pickup (See Figure 13). The internal resonances of the blades were then compared to one another to make sure there were no blades that significantly differed from the rest. This measurement was periodically repeated throughout the tuning process to make sure balance was maintained. Once all of the individual stresses were balanced, an initial transfer function was measured to obtain the resonance frequency of the GAS filter as a reference for later measurements (See Resonance Tuning Data section).

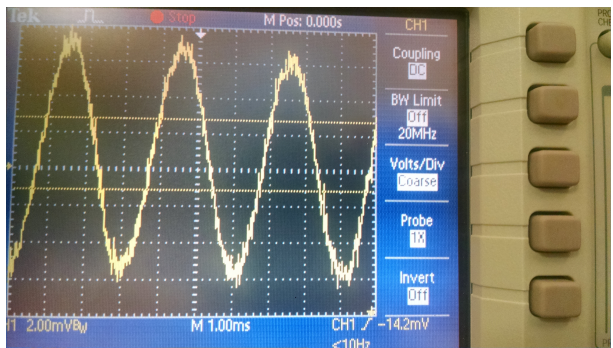
The initial tuning procedure was to turn each of the screws that compress the blades  $1/2$  of a full turn. After turning all of the screws, a transfer function was taken. The function was measured about 15 minutes after all of the screws were turned to allow any motion caused by the activity to significantly decrease. Additionally, our hands were used to help damp the motion as best we could. The filter was tuned using  $1/2$  turns until 4 full turns had been made (See Figure 14, graphs a-g, in Resonance Tuning Data section). However, past 3 turns, the resonance frequency started to rise. This is due to the fact that after the blades have been compressed a certain amount, the anti spring effect becomes too strong. Instead of oscillating around a center point, the blades continue in the direction of a disturbance. After this point was reached, the blades were brought back to the point at which the resonance frequency had been the lowest (3 Turns). From there, the blades were decompressed at either  $1/4$  turns or  $1/6$  turns instead of  $1/2$  turns (See Figure 14, graphs h-m, in Resonance Tuning Data section). Additionally, during the process of decompression, the mass of the payload was changed by small amounts to bring the keystone to a proper height. If the keystone height gets too low or too high, it is indicative of instability. There is an ideal height of the keystone for each compression length at which the resonance frequency is lowest for that compression. The keystone height was brought to this ideal height after each compression/decompression was done. The resonance reached our target of being below .3 Hz at  $11/6$  turns. At this point, the resonance was approximately 0.27 Hz (See last graph in Figure 15).



FIG. 12: The screw with the allen key inside of it and the screw to its left are the two screws that are tightened/loosened to radially compress/decompress the blades.



(a) Here the process of measuring the internal resonance of each individual blade is shown. The blade is lightly struck with the allen key and the pickup sends the frequency signal to the oscilloscope.



(b) Here is an example signal sent to the oscilloscope by the pickup.

FIG. 13

## VII. RESONANCE TUNING DATA

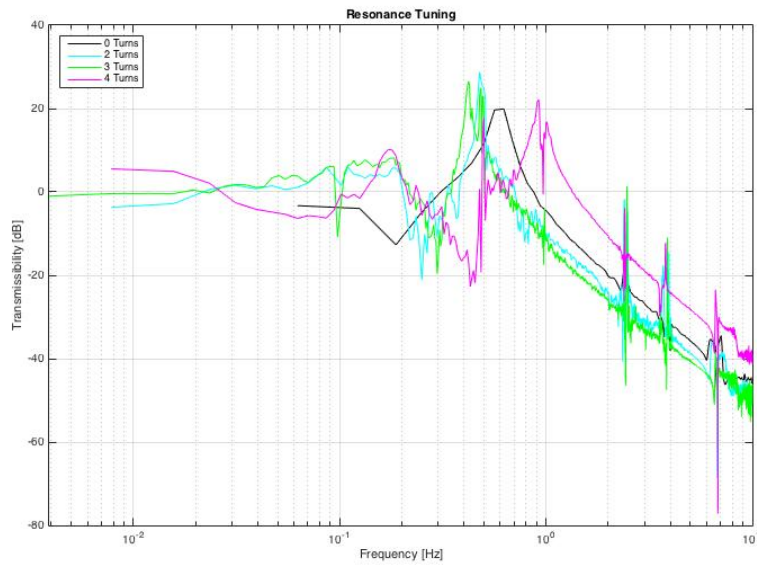


FIG. 14: This graph shows a sample of the measurement taken during the tuning process. Until 3 turns were made, the resonance frequency decreased as expected. After 3 turns, the resonance frequency increased (magenta line). This was due to instability of the system as the GAS effect became too strong.

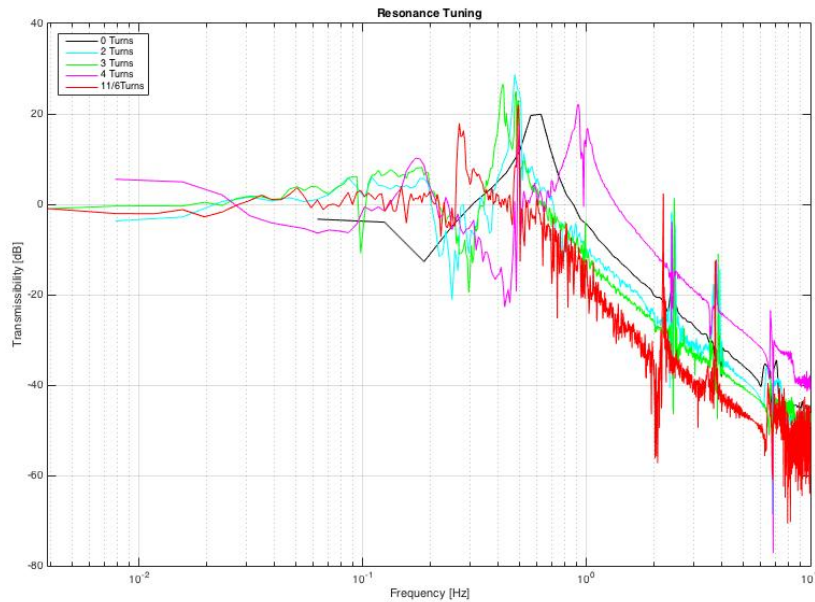


FIG. 15: After making 4 turns, I brought the blades back to the point of lowest resonance (3 turns). From there, the blades were slowly decompressed in 1/6 turns. This time more attention was paid to the height of the keystone and the mass of the payload. Through this method, a resonance frequency of approximately .27Hz was achieved (red line).

## VIII. CENTER OF PERCUSSION TUNING

The center of percussion effect (See Figure 15) causes a saturation in the transfer function of the GAS filters at high frequencies. This effect is due to the moment of inertia of the blade springs. In order to compensate for this effect, magic wands (See Figure 16) are put in the GAS filter. These magic wands are silicon carbide rods that are attached to the GAS filter. Each rod has a small, movable weight at its end used to move the center of percussion of the blades. Silicon carbide is used because it is more stiff than steel. The magic wands are tuned by moving the counterweight until the center of percussion of the blade spring is as close to the clamp point as possible. The incident force on the GAS filter (the motion of the ground due to seismic activity) will act on the clamp point of the blade springs. Therefore, if the center of percussion is anywhere other than the clamp point, extra movement of the keystone is caused by the inertia of the blade. The saturation at high frequencies cannot be completely removed by the magic wands. However, the height of the isolation plateau can be significantly reduced. The process of center of percussion tuning is conducted using the subwoofer. The GAS filter with the wands is excited at higher frequencies (10-100Hz) and the weights are moved until in the ideal location (See Figure 18). At the beginning of the tuning process, the center of percussion was largely overcompensated for. This can be seen by the downward spike before the isolation plateau. Ideally, a smooth transition to a plateau at approximately -80 dB should be seen (See Figure 17).

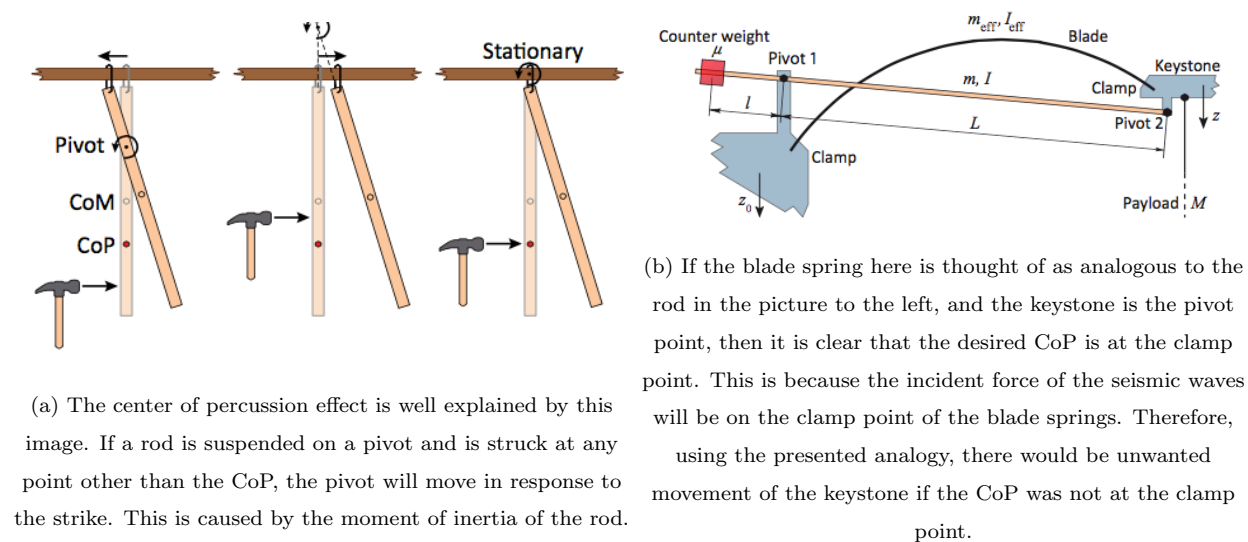


FIG. 16

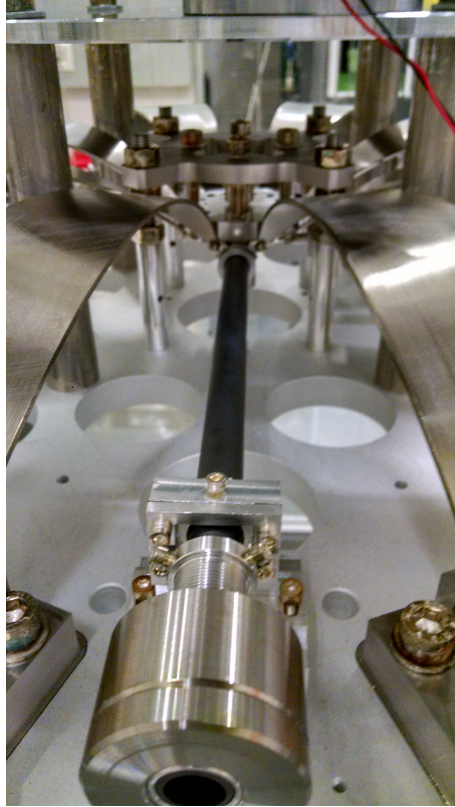


FIG. 17: This is a picture of one of the magic wands. This cylinder on the end is the weight and it is tuned by turning it on the threaded rod that goes through its center

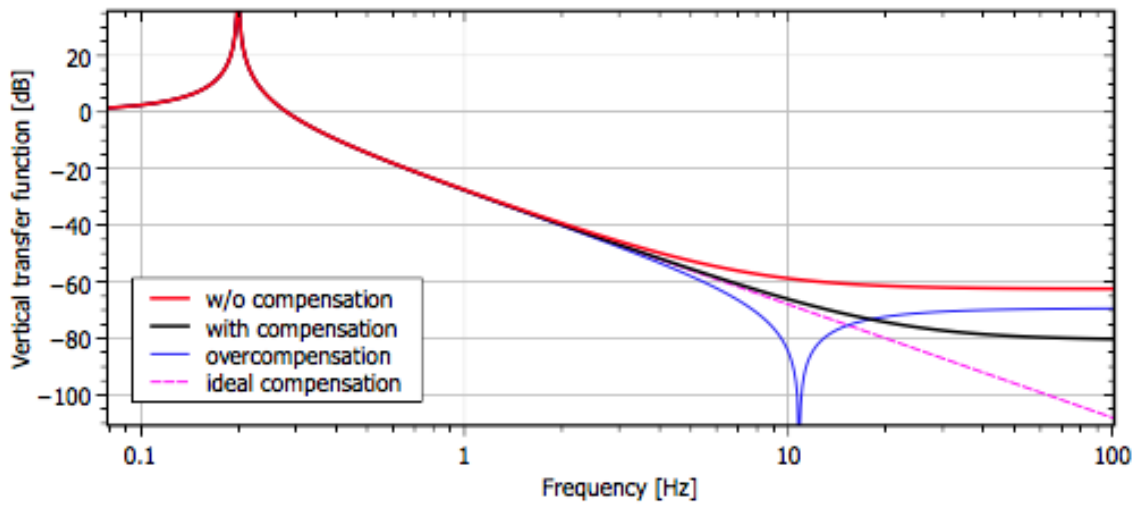


FIG. 18: This graph shows what we are trying to achieve through the CoP tuning. We would like our final result to resemble the black line in this graph.

## IX. CENTER OF PERCUSSION DATA

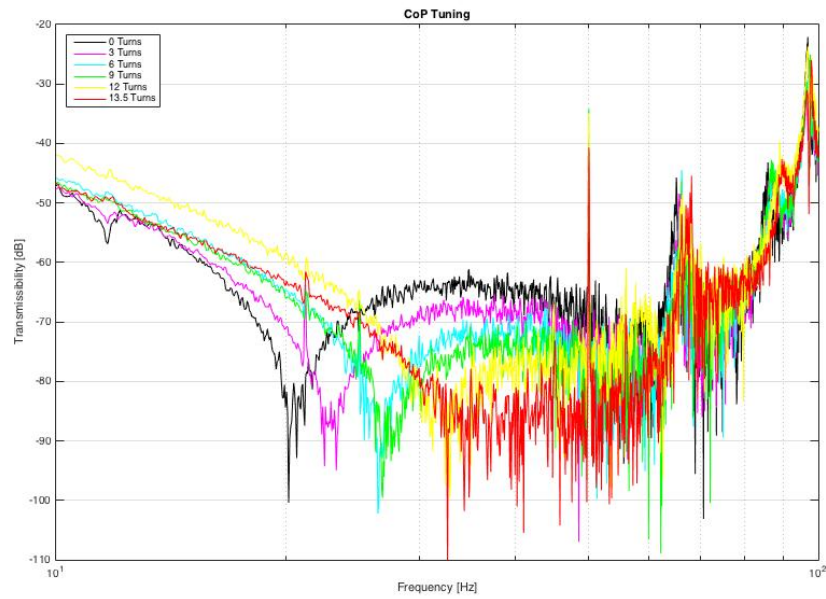


FIG. 19: Shown here is a sample of the measurement made during the center of percussion tuning process. The best isolation plateau was seen at 13.5 turns (red line) at approximately -85dB. The increase in the transfer function at the higher frequencies is due to resonances of the shaker stand.

## **X. ACKNOWLEDGEMENTS**

I would like to thank everyone in the 10m Prototype group and the AEI for making this a very comfortable, informative and fun experience for me. This includes, but is not limited to, Gerald Bergmann, Harald Lück, Vaishali Adya, Janis Woehler, David Wu, Sina Köhlenbeck, Manuela Hanke, Justis Schmitt, Andreas Weidner, and Varun Srivastava. This being my first time away from my family for an extended period of time, I was unsure of my ability to be comfortable. I found that with this group that did not present an issue. I would also like to thank all of the University of Florida staff involved in planning this IREU. I would mainly like to thank Guido Mueller, Bernard Whiting and Kristin Nichola for putting in the effort to make our living arrangements comfortable, working around all of our schedules at once, and organizing this experience. Special thanks are in order for Gerald Bergmann, who took time out of his schedule to oversee my project, show me around the AEI, and answer my plethora of questions. I also give thanks to the NSF for funding this excellent opportunity. I wish the best of luck to all of the members of the group.

## XI. WORKS CITED

1. "gravity wave". Encyclopdia Britannica. Encyclopdia Britannica Online. Encyclopdia Britannica Inc., 2015. Web. 06 Jul. 2015 |<http://www.britannica.com/science/gravity-wave-physics>.
2. Abbott, B P. "LIGO: the Laser Interferometer Gravitational-Wave Observatory." *iop-science*. IOP Publishing. 2009. Web. 7 July 2015.
3. LIGO Scientific Collaboration. "Gravitational Waves: Ripples in the Fabric of Space-time." n.p. n.d. Web. 7 July 2015
4. Wanner, Alexander. "Seismic Attenuation System (AEI-SAS) for the AEI 10m Prototype." Diss. Leibniz University. 2013. Print.
5. Wanner, A. "Seismic attenuation system for the AEI 10 meter Prototype" *iopscience*. IOP Publishing. 2012. Web. 7 July 2015.
6. Beccaria M. "The creep problem in the VIRGO suspensions: a possible solution using Maraging steel." *Nuclear Instruments and Methods in Physics Research A* 404 (1998): 455-469. Print.
7. "Hydrogen Embrittlement." *Corrosion Doctors*. n.d. Web. 29 July 2015
8. "coherence". Encyclopdia Britannica. Encyclopdia Britannica Online. Encyclopdia Britannica Inc., 2015. Web. 29 Jul. 2015 |<http://www.britannica.com/science/coherence>.